Analecta Technica Szegedinensia
Vol. 13, No. 1 ISSN 2064-7964 2019

EFFECTS OF EXTERNAL DISTURBANCES ON THE PERFORMANCE OF AN AXIAL COOLING FAN

Dániel Dorogi, Betti Bolló, Szilárd Szabó
Department of Fluid and Heat Engineering, University of Miskolc, Miskolc, Hungary
e-mail: aramdd@uni-miskolc.hu

ABSTRACT

In this study flow around an axial flow fan is investigated by the means of CFD computations using the commercial software package, ANSYS Fluent. The rotation speed of the impeller was set to the constant value of n = 2500min-1. The results obtained from the computation are validated against those from measurements; good agreements can be seen. The effects of two different external disturbances are analysed. First, the fan was place into a uniform stream where the free stream velocity is varied between U = 0 and 100 km/h. After that, a computation is carried out for U = 0 km/h where the half of the suction side of the fan was covered by a flat plate. The results showed that the fluid pressure and the aerodynamic force increases with the free stream velocity. Asymmetric pressure and fluid force distribution was identified when suction side of the fan was partially covered.

Keywords: aerodynamic forces, CFD, covering, fan, free stream velocity

1. INTRODUCTION

Nowadays, modelling of fluid flow in an axial flow fan is a common engineering problem. Using the available commercial software packages this problem can be handled.
Two types of noise are emitted from the cooling fan of an automotive engine: tonal and broadband noises. Many researchers have studied how these kinds of noises can be reduced [1, 2]. Park and Lee [1] investigated the source of broadband noise from a shrouded automotive cooling fan using a hybrid approach. The calculation of the noise generated by the fan required a large computational domain. A hybrid mesh was created on the geometry consisting 5.2 million cells. The turbulent flow around the fan was modelled by the k-ω SST turbulence model and the noise was predicted using the generalized acoustic analogy of Ffowcs Williams and Hawkings [3]. In order to reduce the computational cost, for first, Park and Lee [1] carried out steady state computations. Once the residual errors decreased to the convergence criteria, they continued the computations considering unsteady flow field.
The computational time is greatly increased by modelling the entire fan unit. If the geometrical properties of the impeller blades are the same and the spacing is constant, it is possible to examine the flow around only one blade section using periodic boundary conditions. Pogorelov et al. [4] used Large Eddy Simulation (LES) and investigated the effect of the gap between the rotating and the stationary parts of the fan. They found that by reducing the tip-gap width, the amplitude of tip-gap vortex wandering is decreasing and the frequencies of the dominant modes are increasing. They also found that tip-gap vortex shedding play an important role in the noise generation.
Lallier-Daniels et al. [2] analysed the acoustic properties of a cooling fan module using Lattice-Boltzmann Method (LBM). The results from the CFD computations were compared with their measurement results obtained using a microphone placed in front of the fan. The comparison between the numerical and experimental results showed good agreements.
Ambdekar et al. [5] investigated the flow structures in a cooling fan using the commercial software package ANSYS Fluent. They investigated the velocity and pressure fields inside the fan, the uniformity of flow in the outlet, the separation zones, the possible locations of cavitation and the noise load.

DOI: 10.14232/analecta.2019.1.48-55

In this paper three-dimensional flow around an axial cooling fan is investigated using the commercial CFD software package, ANSYS Fluent. The results obtained using the currently applied computational approach is validated against measurement results. After the code validation, simulations are carried out using two types of external disturbances. First, the axial fan is placed into a uniform flow. The effects of free stream velocity ranging between U = 0 and 100 km/h are analysed. After that, with zero free stream velocity U = 0 km/h, the half of the suction side of the fan is covered using a flat plate. Three components of fluid force acting on the blade sections are computed and the pressure distribution on the impeller is shown.

2. COMPUTATIONAL SETUP

In this study three-dimensional, incompressible, Newtonian fluid flow around an axial flow fan is modelled using the commercial software package ANSYS Fluent. Three components of the Navier-Stokes equations and continuity equation are solved. Based on the studies of [5–7], Reynolds stresses are approximated using the realizable k-ε turbulence model. The rotating motion of the impeller is modelled using the sliding mesh method.

A schematic diagram of the computational domain is shown in Fig. 1. The axial fan is placed into a channel which height, downstream and upstream length and width are set to 0.804 m, 2.349 m, 2.378 m and 1.2 m, respectively. A cover (flat plate) is placed on the suction side of the fan which is divided into 13 sub-surfaces. These wall surfaces can be ‘activated’ or ‘inactivated’ during computations. In case a sub-surface is activated, no-slip boundary conditions are satisfied on it, otherwise, air can flow through it.

Dirichlet-types of boundary conditions are applied for the three velocity components on the solid surfaces of the fan and in the inlet cross-section. In the inlet uniform stream is prescribed by giving the free stream velocity U. Neumann-types of boundary conditions are used for fluid pressure and for the velocity components in the outlet cross-section.

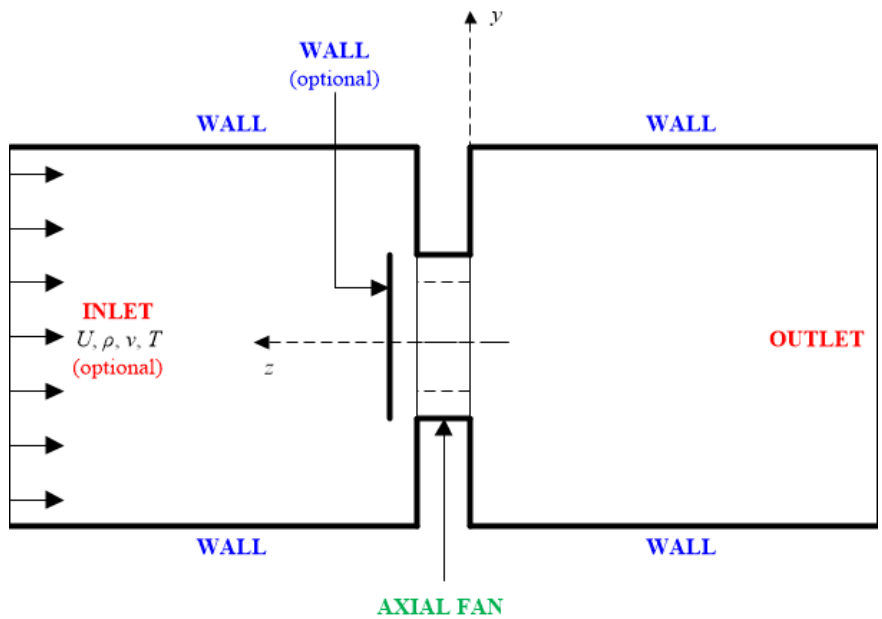

Figure 1. The schematic diagram of the computational domain

DOI: 10.14232/analecta.2019.1.48-55

Figure 2 shows the numerical grid created on the computational domain. It can be seen that the radial cells are logarithmically spaced, providing a fine grid scale near the solid bodies and relatively coarse grid in the far field. The mesh contains approximately 58 million cells.

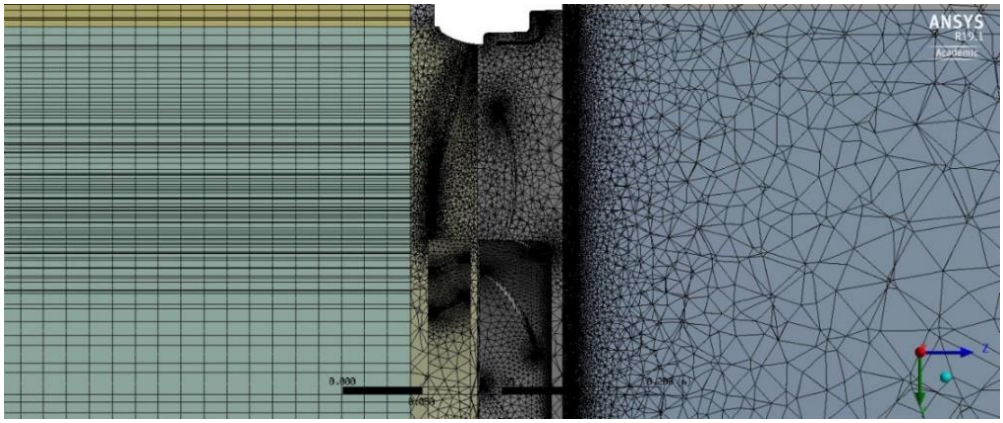

Figure 2. Mesh

The governing equations with the boundary conditions are solved using finite volume method. Second order upwind scheme was used to discretize the convective terms in the momentum equations. The Semi-Implicit Method for the Pressure Linked Equations (SIMPLE) scheme is applied for the pressure-velocity coupling.

3. CODE VALIDATION

Firstly, the results from the applied computational method are validated against experimental results. For this investigation the flat plate on the suction side of the axial fan is inactivate and the rotation speed of the impeller and the free stream velocity in the inlet cross-section are set to n = 2500 min-1 and U = 0 km/h, respectively. For this rotation speed value the revolution time is under t_{rev} = 60/2500 = 0.024 s. The impeller is turned by 5° in each time step, that is, the time step was chosen to be Δt = 0.0003s.

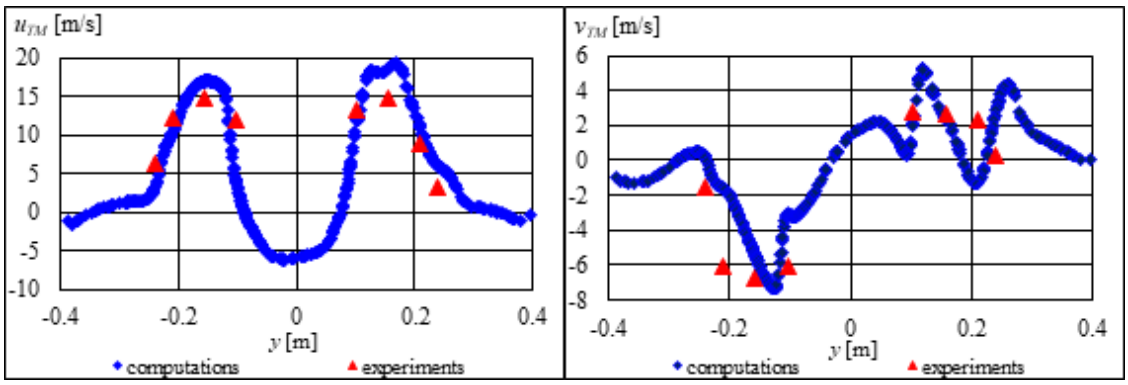

(a) (b)

Figure 3. Comparison between computational and experimental results using the time mean values of u and v velocity components

DOI: 10.14232/analecta.2019.1.48-55

Experiments are carried out using Constant Temperature Anemometry (CTA) technique. During the measurements the time series of u and v velocity components are measured at eight distinct points along the y axis (shown in Fig. 1), $\Delta z = 0.1$ m away from the fan on the pressure side. The sampling frequency was set to 1 kHz and 30s measurement time (in each point) was considered.
In Fig. 3a and b the comparison between the computational and experimental results using the time-mean values of u and v velocity components (u_{TM} and v_{TM}) are shown. It can be seen that the agreements are relatively good, the data sets are in an acceptable tolerance.

4. RESULTS AND DISCUSSION

After the code validation, computations are carried out to investigate the effects of the free stream velocity and the covering surface placed on the suction side of the fan. The rotation speed was set to n = 2500 min-1 similar to that in the validation procedure. During the investigations the three components (in Cartesian coordinate system) of the aerodynamic force (F_x, F_y and F_z) acting on the fan blades and the pressure distribution on the impeller are investigated.

4.1. The effects of free stream velocity

In Fig. 4a and b F_x and F_y aerodynamic force components acting on the blade sections are shown for the free stream velocity values of U = 0, 35, 70 and 100 km/h. The identification numbers of each blade are shown in Fig. 5. It can be seen that these force components can be either greater than and lower than zero for an arbitrary free stream velocity value. In case F_x or F_y is negative the force acts opposite to the rotating direction of the impeller, while for $F_x > 0$ or $F_y > 0$ the force acts in the direction of rotation. It can also be seen that F_x and F_y for U = 70 and 100 km/h increase and decrease at the same locations, so that the force components for these two U values are 'in-phase'. In contrast, the calculated F_x and F_y values for U = 35 km/h are out of phase with those at U = 70 and 100 km/h.
In Fig. 4c the aerodynamic force component in the axial direction F_z is shown for the aforementioned free stream velocity values. It can be seen that F_z is significantly greater than F_x and F_y which is expected. Surprisingly, F_z can also be positive and negative. For positive and negative values the force acts in and opposite to the direction of the main stream, respectively.
In Fig. 5 the pressure distribution on the impeller of the fan is shown for the investigated free stream velocity values. It can be seen that the pressure increases with U which can cause increasing aerodynamic forces on the blades. This statement is true for U > 35 km/h, while at the range of U < 35 km/h additional investigations are required. It is also shown in the figure that the pressure on the pressure side of the fan is always lower than that on the suction side which is also expected.

DOI: 10.14232/analecta.2019.1.48-55

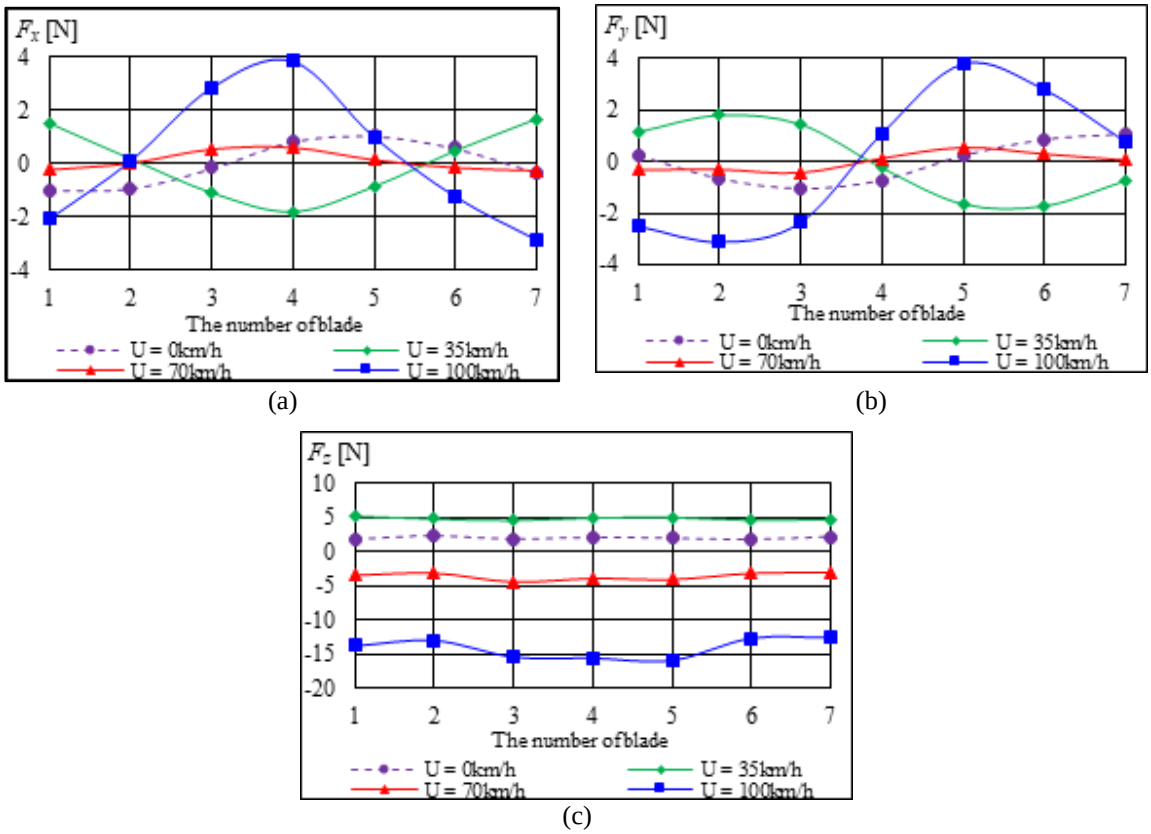

Figure 4. Fx (a), Fy (b) and Fz (c) aerodynamic force components acting on the blade sections.

DOI: 10.14232/analecta.2019.1.48-55

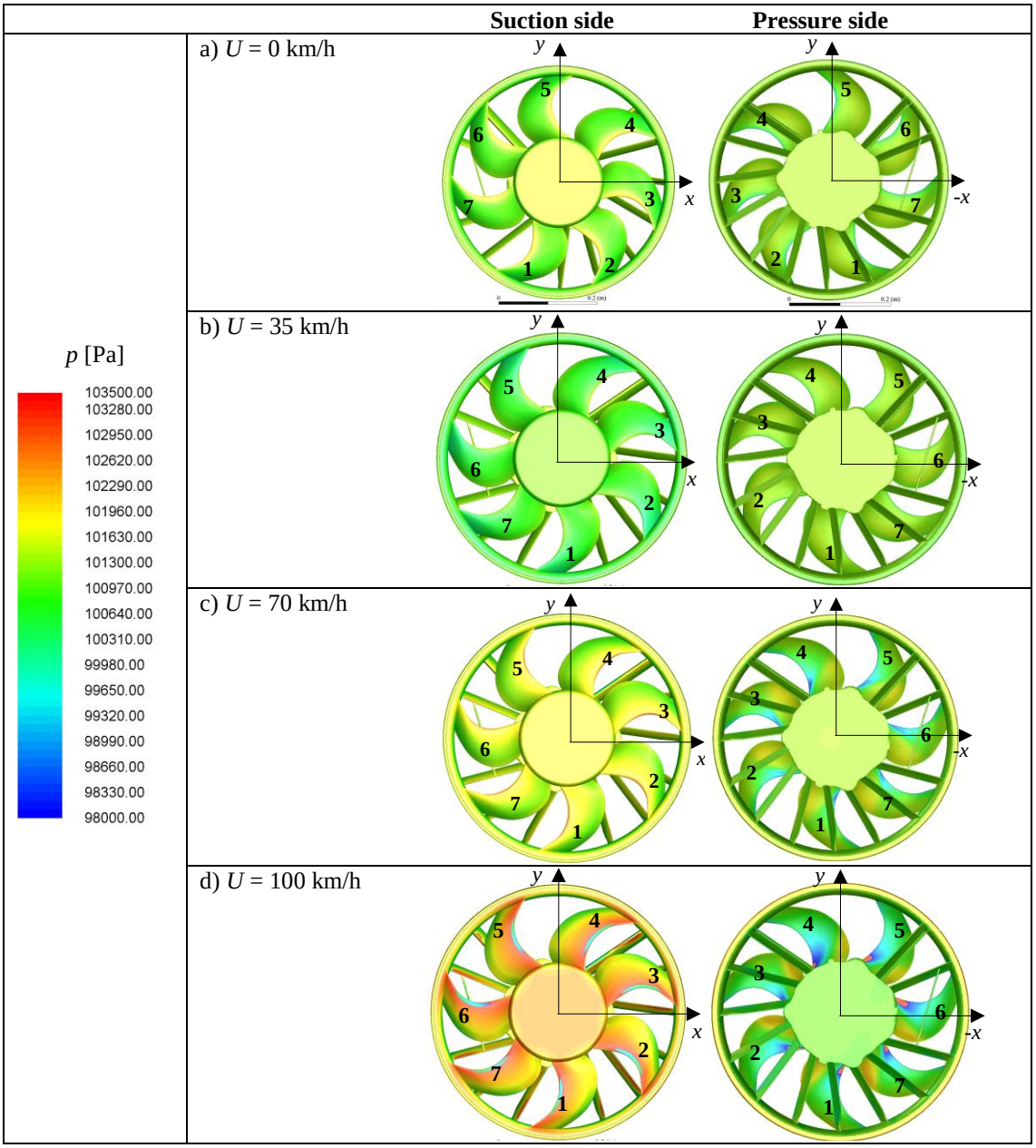

Figure 5. Pressure distribution on the blades for U = 0 km/h (a), 35 km/h (b), 70 km/h (c) and 100 km/h (d)

4.2. The effects of covering plates

Computation is also carried out to investigate the effects of covering on the aerodynamic forces acting on the blades and pressure distribution on the impeller. In this computation the half of the covering surface is 'activated' and the free stream velocity in the inlet cross section is set to zero.

DOI: 10.14232/analecta.2019.1.48-55

Figure 6 shows F_x, F_y and F_z force components acting on the blades of the fan. In Fig. 7 pressure distribution on the impeller of the fan is shown. It is seen in Fig. 7 that blades 2, 3 and 4 are fully covered, blade 5 is partially covered and blades 6, 7, 8 and 1 are free of cover. The force component in the axial direction F_z is the greatest (see Fig. 6) which agrees with the results of the previous computations. As seen in Fig. 6 the forces are higher on those blade sections which are behind the covering plate. This means an asymmetric load on the structure which can possibly induce mechanical vibrations of the structures. This asymmetry can also be seen in Fig. 7.

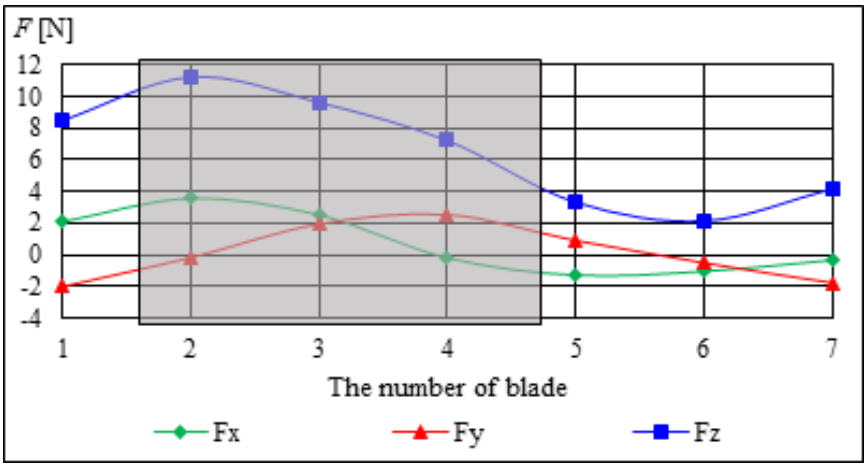

Figure 6. F_x, F_y and F_z force components for cover

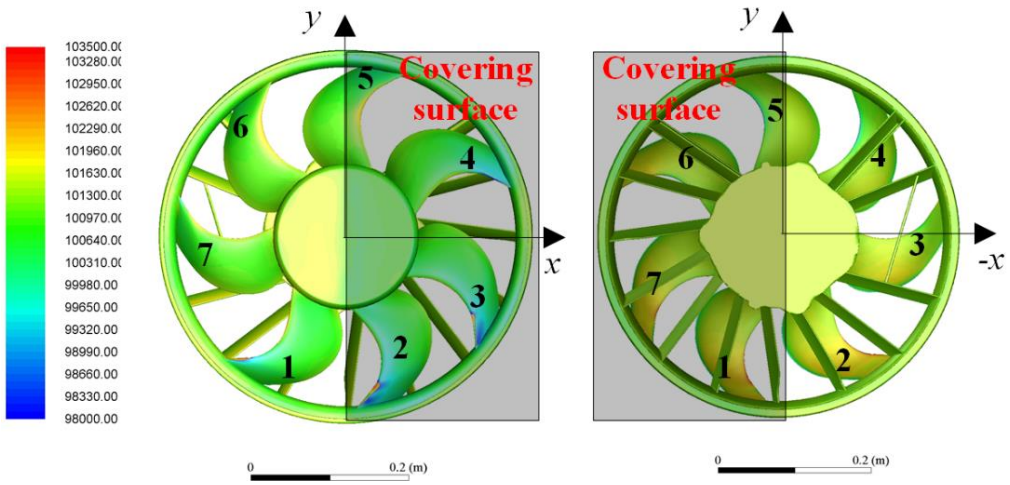

Figure 7. Pressure distribution on the blades for cover

DOI: 10.14232/analecta.2019.1.48-55

4. CONCLUSIONS

In this study fluid flow around an axial cooling fan is investigated by means of numerical simulations using the commercial CFD software package, ANSYS Fluent. The rotation speed of the fan was set to a constant value of n = 2500 min^{-1}. The fan is placed into a uniform stream; the free stream velocity is varied between U = 0 and 100 km/h. A covering flat plate is placed on the suction side of the fan which can be 'activated' (satisfying no-slip boundary conditions on the surface) or 'inactivated' (the fluid can flow through it). The three components of aerodynamic force are evaluated on the blade sections. The results obtained are concluded in the following points:

- The results from the computational method are validated against experimental results (using CTA measurement approach) using the time-mean values of u and v velocity components. The comparison between CFD and measurement data showed good agreements;
- Increasing the free-stream velocity, the fluid forces are showed to increase. F_x and F_y can be either positive and negative meaning that the force acts in or opposite to the rotating direction of the impeller. F_x and F_y values for U > 35 km/h increase and decrease in the same location, so that these data sets are 'in-phase'. At the range of U < 35 km/h different tendencies can be seen that need additional computations. It was shown that axial fluid force components F_z is the highest which can also be positive and negative;
- Asymmetric pressure distribution can be seen on the impeller in case the covering flat plate placed on the suction side of the fan is activated. This asymmetry occurs also in the aerodynamic forces; F_x, F_y and F_z are higher on those blades which are behind the cover and lower on those blades which are free of cover.

ACKNOWLEDGEMENTS

This research was supported by the European Union and the Hungarian State, co-financed by the European Regional Development Fund in the framework of the GINOP-2.2.1-15-2017-00090 project, titled „E-mobility from Miskolc: Improvement of Coolant Pump and Engine Cooling Fan Taking into Account the Higher Quality Requirements in Electric Vehicles".
The research was also supported by the EFOP-3.6.1-16-00011 "Younger and Renewing University – Innovative Knowledge City – institutional development of the University of Miskolc aiming at intelligent specialisation" project implemented in the framework of the Széchenyi 2020 program. The realization of these two projects is supported by the European Union, co-financed by the European Social Fund.

REFERENCES

[1] M. J. Park, D. J. Lee, Sources of broadband noise of an automotive cooling fan, Applied Acoustics 118, 2017, 66–75.
[2] D. Lallier-Daniels, M. Piellard, B. Coutty, S. Moreau, Aeroacoustic study of an axial engine cooling module using lattice-Boltzmann simulations and the Ffowcs Williams and Hawkings' analogy, European Journal of Mechanics B/Fluids, 61, 2017, pp. 244–254.
[3] J. E. Ffowcs Williams, D. L. Hawkings, Sound generation by turbulence and surfaces in arbitrary motion, Philosophical Transactions of the Royal Society of London. Series A, Mathematical and Physical Sciences, 264, 1969, pp. 321–342.
[4] A. Pogorelov, M. Meinke, W. Schröder, Effects of tip-gap width on the flow field in an axial fan. International Journal of Heat and Fluid Flow, 61, 2016, pp. 466–481.
[5] T. C. Ambdekar, S. B. Barve, B. S. Kothavale, N. T. Dhokane, Design and analysis of engine cooling fan, International Journal of Current Engineering and Technology 3 (special issue, 2014), pp. 114-118.
[6] X. Ye, P. Li, C. Li, X. Ding, Numerical investigation of blade tip grooving effect on performance and dynamics of an axial flow fan, Energy, 82, 2015, pp. 556–569.
[7] L. Zhang, Y. Jin, Y. Jin, Effect of Tip Flange on Tip Leakage Flow of Small Axial Flow Fans, Journal of Thermal Science, 23, 2014, pp. 45–52.